

Preparation of Imidazolin-2-iminato Molybdenum and Tungsten Benzylidyne Complexes: A New Pathway to Highly Active Alkyne Metathesis Catalysts

Birte Haberlag,^[a] Xian Wu,^[a] Kai Brandhorst,^[b] Jörg Grunenberg,^[b]
Constantin G. Daniliuc,^[a] Peter G. Jones,^[a] and Matthias Tamm*^[a]

Abstract: The reaction of $[\text{PhC}\equiv\text{MBr}_3(\text{dme})]$ ($\text{dme} = 1,2\text{-dimethoxyethane}$) with the hexafluoro-*tert*-butoxides LiX or KX [$\text{X} = \text{OC}(\text{CF}_3)_2\text{Me}$] afforded the benzylidyne complexes $[\text{PhC}\equiv\text{MX}_3(\text{dme})]$ (**2a**: $\text{M} = \text{W}$, **2b**: $\text{M} = \text{Mo}$), which further reacted with the lithium reagent $\text{Li}(\text{Im}^{\text{tBu}}\text{N})$, generated with MeLi from 1,3-di-*tert*-butylimidazolin-2-imine ($\text{Im}^{\text{tBu}}\text{NH}$), to form the imidazolin-2-iminato complexes $[\text{PhC}\equiv\text{MX}_2(\text{Im}^{\text{tBu}}\text{N})]$ (**3a**: $\text{M} = \text{W}$, **3b**: $\text{M} = \text{Mo}$). The propylidyne complex $[\text{EtC}\equiv\text{MoX}_2(\text{NIm}^{\text{tBu}})]$ (**4**) was obtained by treatment of **3b** with an excess of 3-hexyne.

Complexes **3a** and **3b** are able to efficiently catalyse alkyne cross metathesis of various 3-pentynyl benzyl ethers **5** and benzoic esters **7** at room temperature, to afford 2-butyne and the corresponding diethers **6** and diesters **8**. The tungsten complex **3a** proved to be a superior catalyst for ring-closing alkyne metathesis, and the [10]cyclophanes **10** and **12** were synthesised in high yield from 1,3-bis(3-pentynyloxymethyl)ben-

zene (**9**) and bis(3-pentynyl) phthalate (**11**), respectively. The molecular structures of compounds **2a**, **2b**, **3a**, **3b**, **4**, and **12** were determined by single-crystal X-ray diffraction. DFT calculations have been carried out for catalyst systems based on the imidazolin-2-iminato tungsten and molybdenum complexes **3a** and **3b** by choosing the alkyne metathesis of 2-butyne as the model reaction; the studies revealed a lower activation barrier for the tungsten system.

Keywords: alkynes • imines • metathesis • molybdenum • tungsten

Introduction

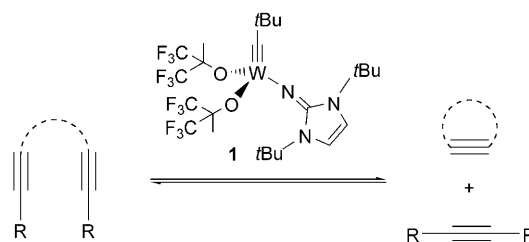
To date, there are only a limited number of catalysts known that efficiently promote the metathesis of alkynes, despite the great potential of catalytic alkyne metathesis as a synthetic tool for the preparation of natural products and highly unsaturated conjugated polymers.^[1] The catalyst systems at hand include: 1) the Mortreux system, consisting of $[\text{Mo}(\text{CO})_6]$ and phenol additives;^[2] 2) Schrock-type tungsten alkylidyne complexes, such as the prototypical neopentyl-

idyne complex $[\text{Me}_3\text{CC}\equiv\text{W}(\text{OCCMe}_3)_3]$;^[3] 3) molybdenum-(III) triamido species based on the Cummins system $[\text{Mo}\{\text{N}(\text{tBu})\text{Ar}\}_3]$;^[4] and, more recently, 4) molybdenum nitride complexes with Ph_3SiO ligands developed by Fürstner.^[5] As a variation of Schrock-type alkylidyne complexes, we have recently introduced imidazolin-2-iminato tungsten neopentylidyne complexes such as **1**,^[6] which display high catalytic activity in alkyne cross metathesis (ACM), ring-closing alkyne metathesis (RCAM) and ring-opening alkyne metathesis polymerisation (ROMP), even at ambient temperature and low catalyst loadings (Scheme 1).^[6,7] According

[a] Dipl.-Chem. B. Haberlag, X. Wu, Dr. C. G. Daniliuc, Prof. Dr. P. G. Jones, Prof. Dr. M. Tamm
Institut für Anorganische und Analytische Chemie
Technische Universität Carolo-Wilhelmina zu Braunschweig
Hagenring 30, 38106 Braunschweig (Germany)
Fax: (+49) 531-391-5309
E-mail: m.tamm@tu-bs.de

[b] Dr. K. Brandhorst, Priv.-Doz. Dr. J. Grunenberg
Institut für Organische Chemie
Technische Universität Carolo-Wilhelmina zu Braunschweig
Hagenring 30, 38106 Braunschweig (Germany)

Supporting information for this article is available on the WWW under <http://dx.doi.org/10.1002/chem.201000597>.



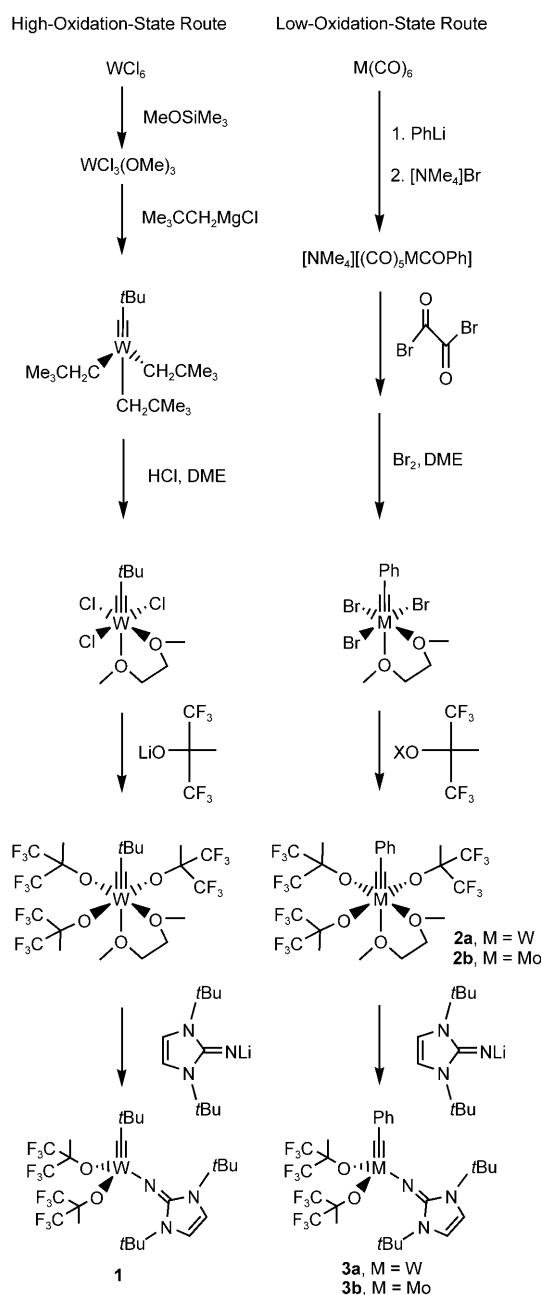
Scheme 1. Catalytic alkyne metathesis with an imidazolin-2-iminato tungsten alkylidyne complex.

to theoretical calculations,^[6a,c,d] the excellent catalytic performance seems to rely on the combination of electron-withdrawing alkoxides, such as hexafluoro-*tert*-butoxide, with strongly electron-donating imidazolin-2-iminato ligands,^[8] to provide a subtle balance between the stability and activity of the resulting tungsten alkylidyne complexes.

Our best and most reliable pre-catalyst, the neopentylidyne complex $[\text{Me}_3\text{CC}\equiv\text{W}\{\text{OC}(\text{CF}_3)_2\text{Me}\}_2(\text{Im}^{\text{tBuN}})]$ (**1**) (Im^{tBuN} = 1,3-di-*tert*-butylimidazolin-2-iminato) was synthesised following the classical high-oxidation-state route,^[6a,d] starting from tungsten(VI) chloride, which requires the use of six equivalents of neopentyl magnesium chloride to afford $[\text{Me}_3\text{CC}\equiv\text{W}(\text{CH}_2\text{CMe}_3)_3]$ by a twofold α -deprotonation.^[3] Subsequently, three more neopentyl equivalents are sacrificed by treatment with ethereal HCl to produce the trichloride $[\text{Me}_3\text{CC}\equiv\text{WCl}_3(\text{dme})]$ (dme = 1,2-dimethoxyethane)^[3b] as the key intermediate for further introduction of the alkoxide and imidazolin-2-iminato ligands (Scheme 2). For us, this protocol proved rather difficult in terms of up-scaling, which was attempted in order to supply larger quantities of the alkyne metathesis pre-catalyst. Consequently, we aimed to develop a low-oxidation-state route starting from $[\text{W}(\text{CO})_6]$, as Mayr et al. used this starting material for the synthesis of the benzylidyne complex $[\text{PhC}\equiv\text{WBr}_3(\text{dme})]$,^[9] which should be equally useful for the subsequent preparation of the benzylidyne analogue of **1**. Naturally, both systems should exhibit similar catalytic activities in alkyne metathesis because the original alkyldiyne moiety is lost during the initiation step. It is therefore the scope of this contribution to give an account of the preparation and structural characterisation of the imidazolin-2-iminato tungsten benzylidyne complex $[\text{PhC}\equiv\text{M}\{\text{OC}(\text{CF}_3)_2\text{Me}\}_2(\text{Im}^{\text{tBuN}})]$ ($\text{M} = \text{W}$, **3a**) together with an investigation of its catalytic performance. In addition, the corresponding molybdenum complex **3b** ($\text{M} = \text{Mo}$) is reported, and its catalytic activity is compared to that of its tungsten congener by means of experimental and theoretical methods.

Results and Discussion

Preparation of imidazolin-2-iminato tungsten benzylidyne complexes: As described by Mayr,^[9a,b] the dark green tungsten tribromo complex $[\text{PhC}\equiv\text{WBr}_3(\text{dme})]$ can be synthesised conveniently from $[\text{W}(\text{CO})_6]$ by reaction with PhLi followed by addition of $[\text{NMe}_4]\text{Br}$, to afford the acyl complex $[\text{NMe}_4][(\text{CO})_3\text{W}(\text{COPh})]$.^[10] This stable intermediate is treated with oxalyl bromide in CH_2Cl_2 at -78°C , resulting in the formation of the Fischer carbyne complex *trans*- $[\text{PhC}\equiv\text{W}(\text{CO})_4\text{Br}]$.^[9,11] Subsequently, decarbonylation and oxidation can be achieved by reaction with Br_2 at -78°C in the presence of 1,2-dimethoxyethane (*dme*), to give $[\text{PhC}\equiv\text{WBr}_3(\text{dme})]$ in approximately 60–70% overall yield. Similarly to the preparation of **1**,^[6a] the fluorinated alkoxides are best introduced at this stage, and the reaction of $[\text{PhC}\equiv\text{WBr}_3(\text{dme})]$ with three equivalents of lithium hexafluoro-*tert*-butoxide, $\text{Li}[\text{OC}(\text{CF}_3)_2\text{Me}]$, in diethyl ether at ambient



Scheme 2. High- and low-oxidation-state routes to tungsten and molybdenum alkyldiyne complexes.

temperature affords the trialkoxide $[\text{PhC}\equiv\text{W}\{\text{OC}(\text{CF}_3)_2\text{Me}\}_3(\text{dme})]$ (**2a**), which can be isolated as orange crystals in 78% yield by recrystallisation from diisopropyl ether (*i*Pr₂O) at -35°C .

The ¹³C NMR spectrum of **2a** shows a characteristic low-field resonance at 278.5 ppm attributable to the alkyldiyne carbon atom, which is slightly upfield from the resonance observed for the corresponding neopentylidyne complex (294.7 ppm),^[12] and falls in the range typically observed for alkyldiyne complexes.^[13] Two broad ¹H NMR resonances at 3.06 and 3.45 ppm are observed for the CH₂ and CH₃ groups of the *dme* ligand, and the ¹⁹F NMR spectrum exhibits only

one singlet at -76.8 ppm, indicating dynamic behaviour of **2a** at room temperature on the NMR timescale. The crystal structure of **2a** was determined by X-ray diffraction analysis; Figure 1 shows an ORTEP diagram of **2a**, confirming

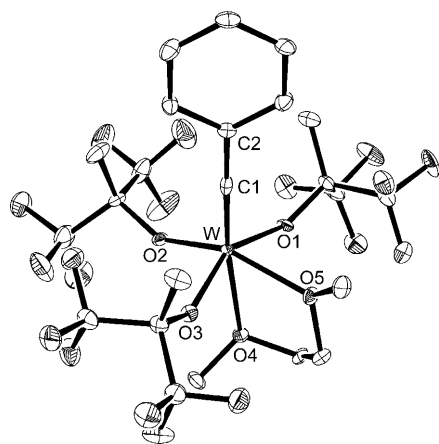


Figure 1. ORTEP diagram of **2a** with thermal displacement parameters drawn at 50% probability. Selected bond lengths [Å] and angles [°]: W–C1 1.761(3), W–O1 1.9554(19), W–O2 1.912(2), W–O3 1.970(2), W–O4 2.3675(19), W–O5 2.217(2); O2–W–O1 95.45(8), O2–W–O3 95.26(8), O2–W–O5 156.08(7), O1–W–O5 79.51(8), O3–W–O5 79.63(8), C1–W–O4 172.46(11), O2–W–O4 82.47(7), O1–W–O4 76.19(7), O3–W–O4 78.19(7), O5–W–O4 73.62(7), C2–C1–W 178.3(2).

the formation of a monomeric tungsten alkylidyne complex that is stabilised by coordination of a chelating dme ligand. The three alkoxides adopt a meridional arrangement around the tungsten atom, giving a strongly distorted octahedral coordination sphere. In fact, the structure is much better described as a square pyramid, with the carbyne carbon atom C1 in the apical position and the oxygen atom O4 capping the basal plane; this is consistent with the observations that the coordinated dme ligand features two distinctly different W–O bond lengths (W–O4 = 2.368(2) Å and W–O5 = 2.217(2) Å) and that the C1–W–O angles containing the four equatorial oxygen atoms O1–O3 and O5 range from 98.88(11)° to 105.04(11)°, thus deviating significantly from the rectangular orientation expected for a regular octahedron. The W–C1 distance of 1.761(3) Å and the W–C1–C2 angle of 178.3(2)° are very similar to the values found for the corresponding neopentylidyne complex.^[6c]

The reaction of **2a** with the lithium reagent (Im^{tBu}N)Li, obtained from the reaction of 1,3-di-*tert*-butylimidazolin-2-imine (Im^{tBu}NH) with methyl lithium, effects the substitution of one hexafluoro-*tert*-butoxide ligand together with the dme solvate molecule, and the formation of the imidazolin-2-iminato benzylidyne complex **3a** as an orange crystalline solid in satisfactory yield (70%). Again, the ¹³C NMR resonance for the carbyne carbon atom in the benzylidyne complex **3a** is observed at higher field (270.6 ppm) compared to that of its neopentylidyne congener **1** (285.6 ppm).^[6a] In agreement with the formation of a configurationally stable C_s-symmetric complex, the ¹³C and ¹⁹F NMR spectra of **3a**

exhibit two quartets each, at 125.7 and 126.2 ppm (¹J_{CF} = 285 Hz), and at -78.2 and -76.4 ppm (⁴J_{FF} = 18 Hz), respectively, for the diastereotopic CF₃ groups. **3a** crystallised in the orthorhombic space group *P*2₁2₁2₁ with three independent molecules in the asymmetric unit; an ORTEP diagram of molecule 1 is shown in Figure 2, confirming the formation

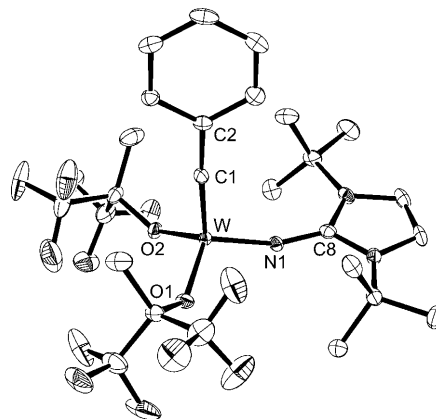


Figure 2. ORTEP diagram of one of the three independent molecules **3a** with thermal displacement parameters drawn at 50% probability. Selected bond lengths [Å] and angles [°] in molecule 1/molecule 2/molecule 3: W–C1 1.759(3), W'–C1' 1.766(3), W''–C1'' 1.765(3), W–N1 1.841(2), W'–N1' 1.842(2), W''–N1'' 1.845(2), W–O1 1.914(2), W'–O1' 1.924(2), W''–O1'' 1.930(2), W–O2 1.930(2), W'–O2' 1.923(2), W''–O2'' 1.916(2); C2–C1–W 175.36(2), C2'–C1'–W' 173.6(2), C2''–C1''–W'' 172.7(2), C1–W–N1 107.89(10), C1'–W'–N1' 107.62(10), C1''–W''–N1'' 107.85(10), C8–N1–W 159.44(18), C8'–N1'–W' 156.22(18), C8''–N1''–W'' 157.55(19).

of a monomeric tungsten benzylidyne complex with a slightly distorted tetrahedral geometry. The W–C distances in the three independent molecules are 1.759(3), 1.766(3), and 1.765(3) Å, respectively, effectively identical to the values found for **1** (1.768(3) and 1.764(3) Å for two independent molecules).^[6a] The W–C–C axes are close to linearity (175.36(19), 173.6(2), 172.7(2)°), whereas considerably smaller W–N–C angles are observed (159.44(18), 156.22(18), 157.56(19)°). Two of the three molecules are closely similar (r.m.s. deviation 0.69 Å); the third differs in the orientation of the CMe(CF₃)₂ group at O2.

Preparation of imidazolin-2-iminato molybdenum benzylidyne complexes:

Because molybdenum complexes are commonly expected to exhibit higher catalytic activities in olefin metathesis than their tungsten congeners,^[1b,i,13] we aimed to prepare molybdenum alkylidyne complexes containing the same combination of electron-withdrawing alkoxides and strongly electron-donating imidazolin-2-iminato ligands as described for the tungsten complexes **1** and **3a**. A high-oxidation-state route would involve the preparation of trialkoxymolybdenum(VI) alkylidyne complexes from [MoO₂Cl₂], as described by Schrock in 1985.^[14] However, the key intermediate [Me₃CC≡Mo(CH₂CMe₃)₃] was synthesised only in low yield (35%),^[15] and therefore we immediately focused on adapting the low-oxidation-state route, out-

lined above for tungsten, to the corresponding molybdenum benzylidyne complexes. Starting from $[\text{Mo}(\text{CO})_6]$, the anionic acyl pentacarbonyl molybdenum complex $[\text{NMe}_4][(\text{CO})_5\text{Mo}(\text{COPh})]$ is obtained after addition of phenyl lithium and $[\text{NMe}_4]\text{Br}$.^[10]

Treatment with oxalyl bromide at -78°C affords the intermediate Fischer carbyne complex *trans*- $[\text{PhC}\equiv\text{Mo}(\text{CO})_4\text{Br}]$, which further reacts with bromine in the presence of dme to give the tribromo complex $[\text{PhC}\equiv\text{MoBr}_3(\text{dme})]$ as a brown crystalline solid in 60% overall yield.^[9a] Subsequently, the use of potassium hexafluoro-*tert*-butoxide, $\text{K}[\text{OC}(\text{CF}_3)_2\text{Me}]$, is required to achieve clean substitution and formation of the trialkoxy benzylidyne complex $[\text{PhC}\equiv\text{Mo}\{\text{OC}(\text{CF}_3)_2\text{Me}\}_3(\text{dme})]$ (**2b**). It should be noted that the latter complex had already been isolated by Schrock from the alkyne metathesis reaction between the neopentylidyne complex $[\text{Me}_3\text{CC}\equiv\text{Mo}\{\text{OC}(\text{CF}_3)_2\text{Me}\}_3(\text{dme})]$ and diphenylacetylene.^[14a] The ^{13}C NMR resonance for the carbyne carbon atom in **2b** is observed at lower field (294.6 ppm) in comparison with **2a**, whereas all other chemical shifts are almost identical. Red single crystals were isolated from *i*Pr₂O solution at -35°C , and the molecular structure of **2b** was determined by X-ray diffraction analysis (Figure 3).

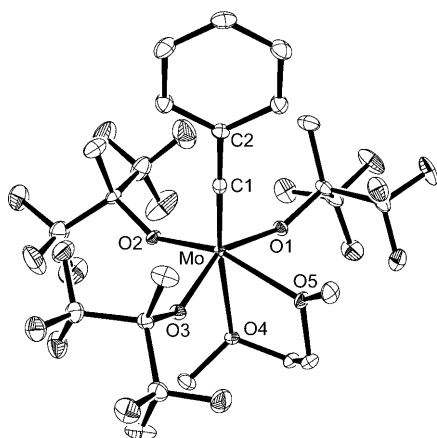


Figure 3. ORTEP diagram of **2b** with thermal displacement parameters drawn at 50% probability. Selected bond lengths [Å] and angles [°]: Mo–C1 1.7555(17), Mo–O1 1.9599(11), Mo–O2 1.9148(11), Mo–O3 1.9697(11), Mo–O4 2.378(11), Mo–O5 2.2487(11); O2–Mo–O1 96.11(5), O2–Mo–O3 95.75(5), O2–Mo–O5 156.72(4), O1–Mo–O5 79.12(5), O3–Mo–O5 79.68(4), C1–Mo–O4 172.01(6), O2–Mo–O4 83.49(4), O1–Mo–O4 76.65(4), O3–Mo–O4 78.84(4), O5–Mo–O4 73.24(4), C2–C1–Mo 178.19(14).

Complex **2b** is isotopic to its tungsten congener **2a**, and, accordingly, the geometries around the metal atoms in **2a** and **2b** are very similar (vide supra). The Mo–C1 distance (1.756(2) Å) is marginally shorter than the corresponding W–C1 distance (1.761(3) Å), which is in agreement with the almost identical ionic radii reported for Mo^{VI} and W^{VI}.^[16]

Finally, the imidazolin-2-iminato ligand can be introduced by substitution of one hexafluoro-*tert*-butoxide ligand together with the dme ligand (Scheme 2), affording **3b** as orange crystals in 60% yield. Again, the spectroscopic data

(^1H , ^{13}C , ^{19}F) of **3b** are almost identical to those observed for its tungsten congener **3a**, with the only exception being the marked downfield shift for the carbyne carbon atom (287.0 ppm). Similarly to the **2a/2b** pair, **3a** and **3b** are isotopic, and, accordingly, **3b** crystallised in the orthorhombic space group $P2_12_12_1$ with three independent molecules in the asymmetric unit; an ORTEP diagram of molecule 1 is shown in Figure 4. Naturally, the structural parameters are very similar to those observed for **3a**, with the Mo–C distances of 1.743(2), 1.742(2) and 1.742(2) Å being slightly shorter than the W–C distances in **3a** (vide supra).

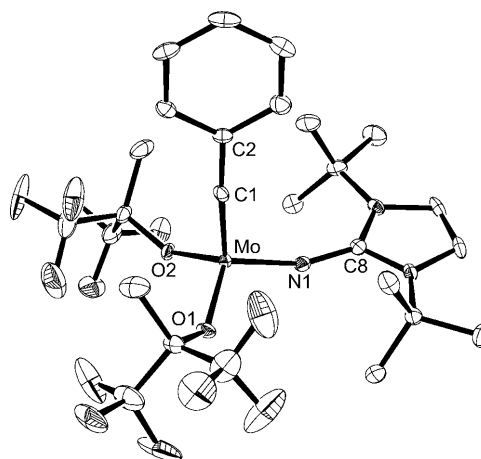


Figure 4. ORTEP diagram of one of the three independent molecules **3b** with thermal displacement parameters drawn at 50% probability. Selected bond lengths [Å] and angles [°] in molecule 1/molecule 2/molecule 3: Mo–C1 1.743(2), Mo'–C1' 1.742(2), Mo''–C1'' 1.742(2), Mo–N1 1.8397(18), Mo'–N1' 1.8444(18), Mo''–N1'' 1.8351(18), Mo–O1 1.9311(15), Mo'–O1' 1.9353(15), Mo''–O1'' 1.9311(15), Mo–O2 1.9448(14), Mo'–O2' 1.9376(15), Mo''–O2'' 1.9379(15); C2–C1–Mo 176.10(18), C2'–C1'–Mo' 174.40(19), C2''–C1''–Mo'' 174.02(18), C1–Mo–N1 106.62(9), C1'–Mo'–N1' 106.05(9), C1''–Mo''–N1'' 106.37(9), C8–N1–Mo 157.55(16), C8'–N1'–Mo' 153.73(16), C8''–N1''–Mo'' 155.57(16).

To investigate the reactivity of **3b** towards alkynes, a hexane solution of **3b** was treated with a tenfold excess of 3-hexyne ($\text{EtC}\equiv\text{CEt}$) at room temperature. The solution was subsequently cooled to -35°C to afford orange crystals, which were subjected to X-ray diffraction analysis. The resulting molecular structure is shown in Figure 5, revealing that the propylidyne complex **4** has formed (Scheme 3). Complex **4** exhibits a slightly distorted tetrahedral geometry; the Mo \equiv C1 triple bond (1.739(4) Å) is shorter, and the Mo–C1–C2 ($171.8(3)^\circ$) and Mo–N1–C4 angles ($149.9(3)^\circ$) are smaller than observed for the benzylidyne complexes **2b** and **3b**. It should be noted that similar reactions employing the tungsten complexes **1** (or **3a**) lead to the clean formation of a metallacyclobutadiene complex with a $\{\text{W}(\text{C}_3\text{Et}_3)\}$ moiety,^[6a] from which the corresponding tungsten propylidyne complex can be obtained by cycloreversion.^[6c] In contrast, we were unable to isolate a stable metallacyclobutadiene intermediate from the reaction of **3b** with 3-hexyne, and this failure is in line with the fact that the formation of

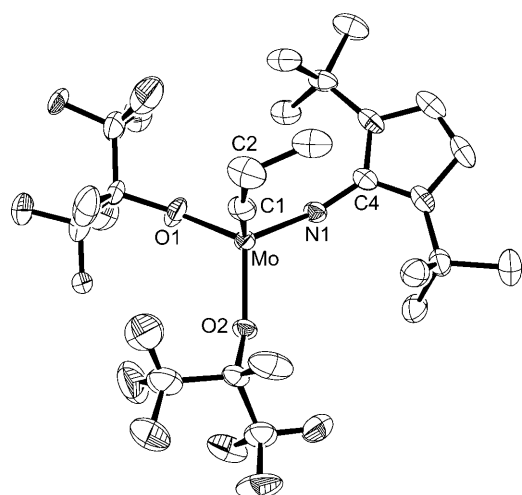
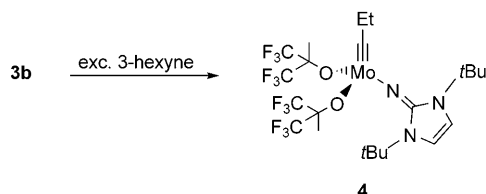


Figure 5. ORTEP diagram of **4** with thermal displacement parameters drawn at 50% probability; the O1–CMe(CF₃)₂ group is disordered over two positions, only one position is shown. Selected bond lengths [Å] and angles [°]: Mo–C1 1.739(4), Mo–N1 1.844(3), Mo–O1 1.950(6), Mo–O2 1.949(2); C2–C1–Mo 171.8(3), C1–Mo–N1 105.83(16), C4–N1–Mo 149.9(3).



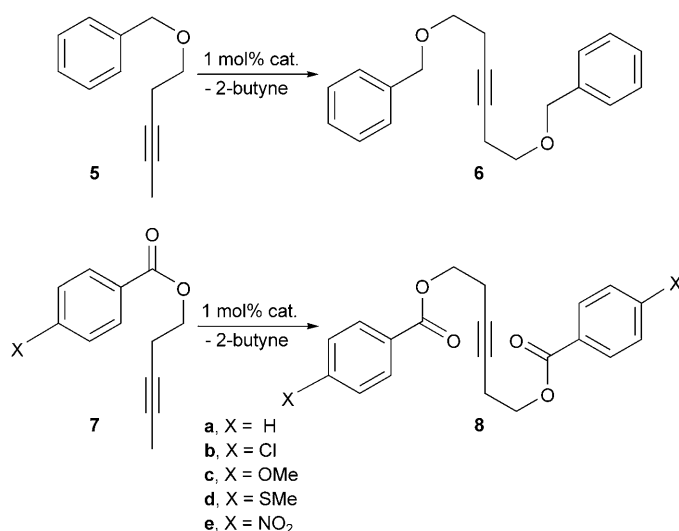
Scheme 3. Reaction of **3b** with an excess of 3-hexyne.

molybdenacyclobutadienes has rarely been observed, and that such species have only been detected by NMR studies.^[14,17] Instead, only the propylidyne complex [EtC≡Mo(NIm^{tBu}){OCMe(CF₃)₂]₂ (**4**) was isolated as orange crystals from the hexane solution.

Catalytic alkyne metathesis with tungsten and molybdenum

alkylidyne complexes: To test the complexes **3a** and **3b** for preparative alkyne cross metathesis (ACM), 3-pentynyl ether **5** was chosen as a model substrate (Scheme 4). In a typical experiment, a toluene solution of **5** and the catalyst (1 mol%) was stirred for 60 min at room temperature under vacuum-driven conditions to remove 2-butyne continuously. Within 10 min intervals, the solvent was completely evaporated, and samples for gas chromatographic analysis were taken after re-addition of the original solvent volume (4 mL). The resulting conversion versus time diagram is shown in Figure 6, and illustrates that both catalysts are active at room temperature and are able to accomplish full conversion within 60 min, despite the observation of a faster initiation rate for the tungsten complex **3a**. After 60 min, the dimer **6** could be isolated in over 90% yield by filtration through alumina and evaporation of the solvent.

Similar results were obtained by using the corresponding 3-pentynyl ester **7a** as the substrate^[48] for catalytic ACM,



Scheme 4. Cross metathesis of the 3-pentynyl ether **5** and esters **7**; reaction conditions: toluene (8 mL), *n*(substrate)=0.5 mmol, *n*(catalyst)=5 μmol (1 mol%), *T*=298 K, *p*≈200 mbar, *t*=1 h; **5**, **7a**, catalyst=**3a** or **3b**; **7b–e**, catalyst=**3a**; yield: **8a** 97%, **8b,c** 98%, **8d** 94%, **8e** 17%.

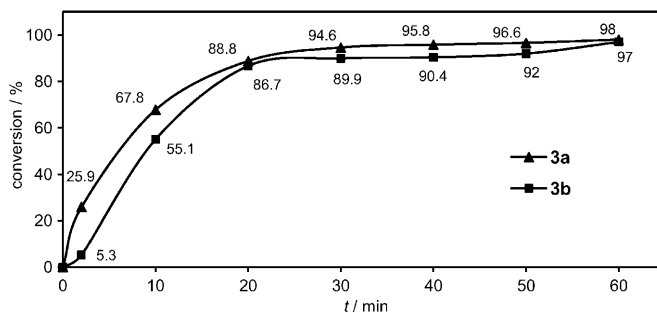
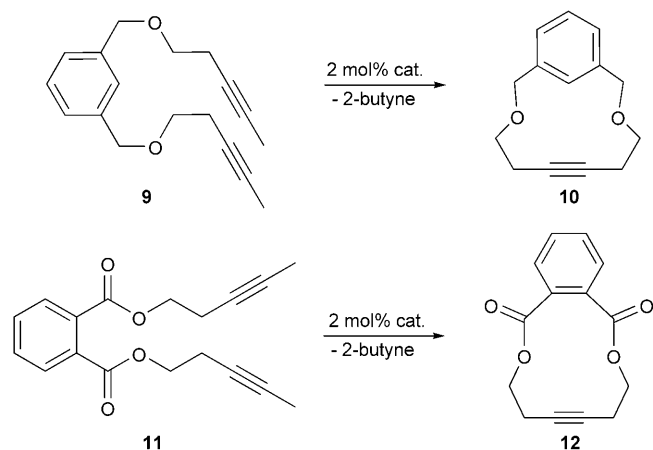


Figure 6. Conversion versus time diagram for the cross metathesis of **5**; reaction conditions: toluene (4 mL), *n*(substrate)=0.5 mmol, *n*(catalyst)=5 μmol (1 mol%), *T*=298 K, reduced pressure. Samples were collected in a stream of argon in less than 3 min. The conversion was monitored by gas chromatography.

and the diester **8a** was isolated in 97% (**3a**) and 95% yield (**3b**). Additionally, the tungsten complex **3a** was used for the cross metathesis of various 3-pentynyl benzoates **7** with various substituents in the 4-position of the phenyl ring. The resulting diesters **8** were isolated in more than 90% yield for X=H, Cl, OMe, and SMe, indicating a promising functional group tolerance for this catalyst system. In contrast, only 17% of the nitro compound **8e** could be obtained in the presence of 1 mol% catalyst loading.^[18] Future studies are necessary to uncover the full range of functional groups that are compatible with our catalyst system.

We have recently demonstrated that the neopentylidyne complex **1** exhibits high catalytic activity in the ring-closing alkyne metathesis (RCAM) of α,ω -diynes such as *o*-, *m*- and *p*-di(3-pentynyloxymethyl)benzenes. Depending on the substitution pattern, different selectivities towards the formation of monomeric [10]cyclophanes or dimeric [10.10]cyclophanes were observed, which could be attributed to the rela-

tive thermodynamic stability of the emerging cycloalkynes.^[7a] In case of the *meta*-diyne **9**, exclusive formation of the [10]-*meta*-cyclophane **10** was observed, and, consequently, this substrate was used for studying the performance of complexes **3a** and **3b** in catalytic RCAM reactions (Scheme 5). A 4.5 mm solution of **7** and the catalyst **3a** or



Scheme 5. RCAM of 1,3-bis(3-pentynyloxymethyl)benzene **9** and bis(3-pentynyl)phthalate **11**; reaction conditions: toluene (4.5 mm), 2 mol% catalyst (**3a** or **3b**), $T = 298$ K, $p = 300$ mbar, $t = 2$ h.

3b (2 mol%) in toluene was stirred for 2 h at room temperature under reduced pressure to remove 2-butene continuously. Filtration through alumina and evaporation of the solvent afforded **10** in 86% isolated yield by using the tungsten catalyst **3a**, whereas only 47% could be obtained for the molybdenum system **3b**, indicating that the latter seems to be a less active catalyst for alkyne metathesis at room temperature than **3a**.

The di(3-pentynyl) phthalate **11** was chosen as a second substrate for RCAM, as theoretical calculations indicate a strong preference for the formation of the [10]-*ortho*-cyclophane **12**.^[19] Under the same conditions as described for **9**, the RCAM of **11** in the presence of catalytic amounts of **3a** or **3b** (2 mol%) afforded the cycloalkyne **12** in excellent yield (98%) in the case of **3a**, whereas, once again, a significantly lower yield (20%) was obtained for **3b** (Scheme 5). **12** was fully characterised by means of spectroscopic methods,^[4d,m] and a single crystal of **12** was additionally subjected to X-ray diffraction analysis. The resulting molecular structure is shown in Figure 7, which confirms unequivocally the formation of a monomeric cycloalkyne, and the existence of an unstrained 12-membered ring. The C4=C5 triple bond length is 1.189(2) Å, and the tilted conformation of the two carboxylic groups is similar to those found for other organic phthalates.^[20]

Theoretical investigation of alkyne metathesis with tungsten and molybdenum alkylidyne complexes: To study the relative catalytic activities of molybdenum and tungsten imidazolin-2-iminato benzylidyne complexes **3a** and **3b** at room

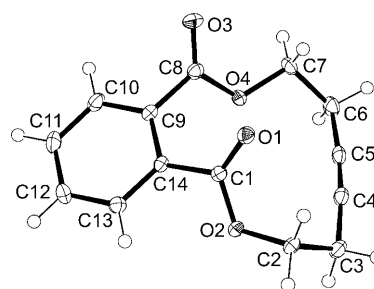
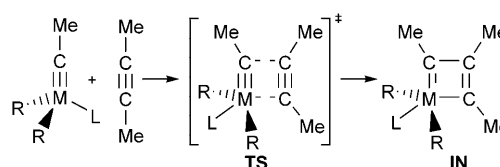


Figure 7. ORTEP diagram of **12** with thermal displacement parameters drawn at 50% probability. Selected bond lengths [Å] and angles [°]: O1–C1 1.2074(18), O3–C8 1.2025(17), C4–C5 1.189(2); O2–C1–C14 111.75(11), O4–C8–C9 110.01(11).

temperature, theoretical calculations using density functional theory (DFT) were performed. Similarly to our previous studies,^[6a,c] the symmetric metathesis of 2-butyne (MeC≡CMe) was chosen as the model reaction (Scheme 6). Based



Scheme 6. Symmetric metathesis of 2-butyne ($R = \text{OCMe}(\text{CF}_3)_2$; $L = \text{Im}^{\text{tBu}}\text{N}$).

on the conventional [2+2] cycloaddition–cycloreversion mechanism,^[21,22] the first three relevant stationary points (catalyst plus 2-butyne, transition state TS, and metallacyclobutadiene intermediate IN) of the rate-determining alkyne metathesis step were characterised for the $[\text{MeC}\equiv\text{WR}_2\text{L}]$ and $[\text{MeC}\equiv\text{MoR}_2\text{L}]$ model systems ($R = \text{OCMe}(\text{CF}_3)_2$, $L = \text{Im}^{\text{tBu}}\text{N}$). It should be noted that a full catalytic cycle additionally involves the interconversion between two metallacyclobutadiene intermediates. However, since this rearrangement has a significantly lower barrier, no attempts were made to locate this second transition state. Table 1 summarises the calculated B3LYP energies and enthalpies. For comparison of these gas-phase computations with our experimental results, it should be noted that, for the associative mechanism at work, entropic effects are expected to be smaller in the condensed phase, which should afford considerably lower free activation barriers.

Table 1. Relative B3LYP energies and enthalpies (in kcal mol⁻¹) for the reaction of selected catalysts with 2-butyne (Scheme 6).^[a]

Catalyst	ΔE_0^\ddagger	TS ^[b]		IN ^[b]		
		ΔH_{298}^\ddagger	ΔG_{298}^\ddagger	ΔE_0	ΔH_{298}	ΔG_{298}
3a M: W	9.78	8.99	26.05	-2.47	-3.54	13.67
3b M: Mo	15.24	14.49	30.10	5.39	4.54	19.98

[a] For details, see the Experimental Section. [b] ΔE_0 : relative energies at 0 K, ΔH_{298} : enthalpies at 298 K, ΔG_{298} : Gibbs free energies at 298 K; all values are given with respect to the isolated catalyst and 2-butyne.

The molybdenum system exhibits a free energy barrier (ΔG_{298}^\ddagger) of 30.10 kcal mol⁻¹, which is 4.05 kcal mol⁻¹ higher than that calculated for the tungsten system (26.05 kcal mol⁻¹) (see Table 1). Assuming a similar frequency factor in the Arrhenius equation for both reactions, this difference ($\Delta\Delta G_{298}^\ddagger$) results in a decrease of the rate constant for the Mo system, which is in line with the observed inferior catalytic behaviour of **3b** as an RCAM catalyst (vide supra). The entropic contributions to ΔG for the W and Mo systems are computed to be 17.06 and 15.61 kcal mol⁻¹, respectively, for the activation barrier (ΔG_{298}^\ddagger), and 17.21 and 15.44 kcal mol⁻¹, respectively, for the formation of the metallacyclobutadiene intermediates (ΔG_{298}°). Accordingly, the differences in ΔG_{298}^\ddagger and ΔG_{298}° are largely enthalpic in nature. The formation of the metallacyclobutadiene intermediate IN is exothermic for the tungsten system ($\Delta H_{298}^\circ = -3.54$ kcal mol⁻¹), whereas the corresponding reaction with the Mo catalyst proceeds endothermically ($\Delta H_{298}^\circ = +4.54$ kcal mol⁻¹), which might be one reason for our inability to isolate a stable molybdenacyclobutadiene from the reaction of **3b** with 3-hexyne (vide supra).

Conclusion

A low-oxidation-state route starting from $[W(CO)_6]$ and $[Mo(CO)_6]$ has been developed to provide convenient and economic access to tungsten and molybdenum imidazolin-2-iminato alkylidyne complexes, which have been designed to catalyse alkyne metathesis reactions efficiently. The resulting W and Mo benzyldiene complexes are both active pre-catalysts for the cross metathesis of aliphatic ether- and ester-functionalised alkynes even at room temperature. However, the tungsten system tends to show a superior performance, particularly in ring-closing alkyne metathesis; this is in line with DFT studies, which predict a higher barrier for the molybdenum-based catalyst system. A similar trend has previously been derived for symmetric model complexes of the type $[MeC\equiv M(OMe)_3]$ (M = Mo, W).^[22] However, additional calculations are required to fully uncover the key factors that control the efficiency of d⁰ alkyne metathesis catalysts.^[23]

Experimental Section

General procedures: All operations were performed in a glove box (MBraun 200B, argon atmosphere) or on a Schlenk line using Schlenk techniques. All solvents were purified and dried by a solvent purification system from MBraun or using standard methods, and stored over a molecular sieve (4 Å). The ¹H, ¹³C, and ¹⁹F NMR measurements were performed on Bruker DPX 200 (200 MHz) and Bruker DRX 400 (400 MHz) devices. The chemical shifts are expressed in parts per million (ppm) using tetramethylsilane (TMS) (for ¹H and ¹³C) and CFCl₃ (for ¹⁹F) as internal standards. Coupling constants (*J*) are reported in Hertz (Hz). Splitting patterns are indicated as s (singlet), d (doublet), t (triplet), q (quartet), m (multiplet) and br (broad). Elemental analysis (C, H, N) was performed by combustion and gas chromatographical analysis using an Elementar varioMICRO. GC analysis was performed on a SHIMADZU

GC-2010, GC-MS on a JOEL AccuTOF, and MS on a Finnigan MAT 95 (EI) and Finnigan MAT 95 (ESI). The compounds $[PhC\equiv WBr_3(dme)]$,^[9b] $[NMe_4][Mo(CO)_3COC_6H_5]$,^[10] and $LiOCCH_3(CF_3)_2$, $Li(NIm^{tBu})$ were prepared according to the literature procedures.^[6a] The preparation of 1,3-bis(3-pentynylloxymethyl)benzene (**9**) was previously reported.^[7a] The procedure for the synthesis of the compounds **5**, **7a–e**, and **11** can be found in the Supporting Information.

Synthesis and characterisation of $[PhC\equiv W\{OCMe(CF_3)_2\}_3(dme)]$ (2a**):** The deep green tungsten benzyldiene complex $[PhC\equiv WBr_3(dme)]$ (400 mg, 0.664 mmol) was added slowly to the lithium alkoxide $Li[OCCH_3(CF_3)_2]$ (374 mg, 1.989 mmol), suspended in diethyl ether (30 mL). The suspension turned brown during the addition, and was stirred for 16 h at ambient temperature, then concentrated and filtered. After removal of the diethyl ether, diisopropyl ether (8 mL) was added and the brown suspension was filtered again. Orange crystals were obtained after keeping the *i*Pr₂O solution at -35 °C for several hours. Yield: 470 mg (78 %); ¹H NMR (400.1 MHz, C₆D₆, 25 °C): $\delta = 1.82$ (s, 9H; $OCCH_3(CF_3)_2$), 3.06 (br, 4H; OCH_2CH_2O), 3.45 (br, 6H; OCH_3), 6.61–6.71 (m, 1H; *p*-CH), 6.87 (m, 2H; *m*-CH), 7.19 ppm (m, 2H; *o*-CH); ¹³C NMR (100.6 MHz, C₆D₆, 25 °C): $\delta = 18.8$ (s, $OCCH_3(CF_3)_2$), 68.2 (s, OCH_2CH_2O), 74.9 (s, OCH_3), 86.9 (s, $OCCH_3(CF_3)_2$), 126.3 (q, CF_3 , $J_{CF} = 289$ Hz), 127.5 (s, CH), 127.9 (s, CH), 128.6 (s, CH), 133.8 (*i*-C), 278.5 ppm ($PhC\equiv W$); ¹⁹F NMR (188.3 MHz, C₆D₆, 25 °C): $\delta = -76.8$ ppm (s, CF_3); elemental analysis calcd (%) for C₂₃H₂₄F₁₈O₅W: C 30.48, H 2.67; found: C 30.49, H 2.80.

Synthesis and characterisation of $[PhC\equiv W(NIm^{tBu})\{OCMe(CF_3)_2\}_2]$ (3a**):** $Li(NIm^{tBu})$ (44.5 mg, 0.221 mmol) was dissolved in toluene (5 mL) and added to $[PhC\equiv W\{OCMe(CF_3)_2\}_3(DME)]$ (200 mg, 0.221 mmol) dissolved in toluene (5 mL). The mixture was stirred at ambient temperature for 15 min, and then concentrated and filtered. The solvent was removed and the product was extracted with hexane (5 mL). Orange crystals were obtained after keeping the hexane solution at -35 °C for several hours. Yield: 128 mg (70 %); ¹H NMR (300.1 MHz, C₆D₆, 25 °C): $\delta = 1.27$ (s 18H; $NC(CH_3)_3$), 1.94 (s, 6H; $OCCH_3(CF_3)_2$), 5.92 (s, 2H; *NCH*), 6.68–6.78 (m, 1H; *p*-CH), 6.93–7.02 (m, 2H; *m*-CH), 7.12–7.22 ppm (m, 2H; *o*-CH); ¹³C NMR (75.5 MHz, C₆D₆, 25 °C): $\delta = 19.9$ (s, $OCCH_3(CF_3)_2$), 28.5 (s, $NC(CH_3)_3$), 57.4 (s, $NC(CH_3)_3$), 83.3 (s, $OCCH_3(CF_3)_2$), 110.3 (s, $NC\equiv CN$), 125.7 (q, $J_{CF} = 285$ Hz, CF_3), 126.2 (q, $J_{CF} = 285$ Hz, CF_3), 127.9 (s, CH), 129.7 (s, CH), 131.8 (s, CH), 148.1 (s, *i*-C), 158.5 (s, NCN), 270.6 ppm (s, $PhC\equiv W$); ¹⁹F NMR (376.4 MHz, C₆D₆, 25 °C): $\delta = -78.2$ (q, $J_{FF} = 18$ Hz, 6F; CF_3), -76.4 ppm (q, $J_{FF} = 18$ Hz, 6F; CF_3); elemental analysis calcd (%) for C₂₆H₃₁F₁₂N₃O₂W: C 37.65, H 3.77, N 5.07; found: C 37.13, H 3.84, N 5.14.

Synthesis and characterisation of $[PhC\equiv MoBr_3(dme)]$: A cold solution (-78 °C) of oxalyl bromide in CH₂Cl₂ was added to a cold solution of $[NMe_4][Mo(CO)_3COC_6H_5]$ (4.25 g, 10 mmol) in CH₂Cl₂. After stirring the suspension for 15 min at -78 °C, it was warmed to -40 °C and then immediately cooled back to -78 °C. The reaction mixture was filtered through Celite at -78 °C. Then ten equivalents of *dme* and a cold solution of Br₂ in CH₂Cl₂ (0.18 mL, 10 mmol) were added to the filtrate at -78 °C and stirred for 45 min. Finally, the solvent was removed in an ice-water bath. The resulting brown solid was taken up in CH₂Cl₂ (20 mL) and precipitated with pentane three times. The final CH₂Cl₂ solution was filtered, and after precipitation with pentane a brown crystalline solid was obtained. Yield: 3.06 g (60 %); ¹H NMR (200.1 MHz, C₆D₆, 25 °C): $\delta = 2.93$ (br, 2H; $MeOCH_2CH_2OMe$), 3.10 (br, 5H; $MeOCH_2CH_2OCH_3$), 3.55 (s, 3H; $CH_3OCH_2CH_2OMe$), 6.64 (m, 1H; *CH*), 6.98 (m, 2H; *CH*), 7.52 ppm (m, 2H; *CH*); elemental analysis calcd (%) for C₁₁H₁₅Br₃O₂Mo: C 25.66, H 2.94; found: C 25.59, H 3.62.

Synthesis and characterisation of $[PhC\equiv Mo\{OCMe(CF_3)_2\}_3(dme)]$ (2b**):** The brown molybdenum benzyldiene complex $[PhC\equiv MoBr_3(dme)]$ (500 mg, 0.97 mmol) was added to the potassium alkoxide $KOCCH_3(CF_3)_2$ (663 mg, 3.01 mmol) suspended in diethyl ether (20 mL). The suspension was stirred for 16 h at RT, and the resulting suspension was filtered and extracted with small amounts of Et₂O. After removal of the solvent, the brown solid was recrystallised from *i*Pr₂O (5 mL) at -35 °C as orange crystals. Yield: 700 mg (88 %); ¹H NMR (400.1 MHz, C₆D₆, 25 °C): $\delta = 1.81$ (s, 9H; $OCCH_3(CF_3)_2$), 3.05 (s, 4H; OCH_2CH_2O), 3.25 (s,

6H; OCH₃), 6.74–6.78 (m, 1H; *p*-CH), 6.91–6.99 (m, 2H; *m*-CH), 7.09–7.16 ppm (m, 2H; *o*-CH); ¹³C NMR (100.6 MHz, C₆D₆, 25°C): δ = 18.7 (s, OCCH₂(CF₃)₂), 63.4 (s, OCH₃), 71.3 (s, OCH₂CH₂O), 83.7 (s, OCCH₂(CF₃)₂), 126.1 (q, *J*_{CF} = 290 Hz, CF₃), 127.6 (s, CH), 129.2 (s, CH), 129.9 (s, CH), 143.5 (s, *i*-C), 294.6 ppm (s, PhC≡Mo); ¹⁹F NMR (188.3 MHz, C₆D₆, 25°C): δ = -76.7 ppm (s, CF₃); elemental analysis calcd (%) for C₂₃H₂₄F₁₈O₂Mo: C 33.76, H 2.96; found: C 33.19, H 3.20.

The potassium salt KOCCH₃(CF₃)₂ was synthesised in advance by treating the corresponding alcohol (3 g; 16.48 mmol) with KH (661 mg; 16.48 mmol) in Et₂O (30 mL). The reaction mixture was stirred for 4 h at RT. Filtration and evaporation of the solvent gave the salt as a white powder.

Synthesis and characterisation of [PhC≡Mo(NIm^{flu})(OCMe(CF₃)₂)] (3b): A suspension of (Im^{flu}N)Li (25 mg, 0.122 mmol) in toluene (2 mL) was added to a solution of the molybdenum benzylidyne complex (100 mg, 0.122 mmol) dissolved in toluene (5 mL). After stirring for 1 h at 40°C the solution was filtered and the solvent removed. The resulting solid was dissolved in *i*Pr₂O (4 mL) and the solution filtered. After keeping the solution at -35°C for several hours orange crystals were obtained. Yield: 55 mg (60%); ¹H NMR (400.1 MHz, C₆D₆, 25°C): δ = 1.27 (s, 18H; NC(CH₃)₃), 1.89 (s, 6H; OC(CH₃)(CF₃)₂), 5.96 (s, 2H; NCH), 6.81–6.84 (m, 1H; *p*-CH), 7.00–7.04 (m, 2H; *m*-CH), 7.10–7.16 ppm (m, 2H; *o*-CH); ¹³C NMR (100.6 MHz, C₆D₆, 25°C): δ = 20.0 (s, OCCH₂(CF₃)₂), 28.6 (s, NC(CH₃)₃), 57.6 (s, NC(CH₃)₃), 110.8 (s, NC=CN), 123.5 (q, *J*_{CF} = 288 Hz, CF₃), 126.3 (q, *J*_{CF} = 288 Hz, CF₃), 127.6 (s, CH), 127.9 (s, CH), 128.2 (s, CH), 128.9 (s, CH), 146.6 (s, *i*-C), 158.0 (s, NCN), 287.0 ppm (s, PhC≡Mo); ¹⁹F NMR (376.4 MHz, C₆D₆, 25°C): δ = -78.3 (q, ⁴*J*_{FF} = 18 Hz, 6F; CF₃), -76.5 ppm (q, ⁴*J*_{FF} = 18 Hz, 6F; CF₃); elemental analysis calcd (%) for C₂₆H₃₁F₁₂MoN₃O₂: C 42.12, H 4.21, N 5.67; found: C 42.01, H 4.20, N 5.52.

Comparison of catalytic activities: In order to compare the catalytic activity of the tungsten and molybdenum benzylidyne complexes **3a** and **3b**, the homodimerisation metathesis reaction of 3-pentynylloxymethylbenzene (**5**) was performed. In a glove box, a 50 mL Schlenk tube was charged with a solution of **5** (0.5 mmol) and the catalyst **3a** or **3b** (5 μmol, 1 mol%) in toluene (4 mL). The Schlenk tube was taken out of the glove box and connected to a Schlenk line. At 10 min intervals, the solvent (together with 2-butyne) was completely evaporated under reduced pressure. With disconnection from the vacuum line for approximately three minutes, samples for gas chromatographic analysis were isolated after re-addition of the original solvent volume (4 mL), and filtered through alumina to remove the catalyst. The first sample was taken directly after the addition of the catalyst to **5** (no vacuum).

General procedure for alkyne cross metathesis: In a glove box, a 50 mL Schlenk tube was charged with a solution of the substrate (0.5 mmol) and the catalyst **3a** (5 μmol, 1 mol%) in toluene (8 mL). The Schlenk tube was taken out of the glove box and connected to a Schlenk line. Reduced pressure (≈200 mbar) was applied, and the solvent (together with 2-butyne) was slowly evaporated over a period of one hour. The residue was re-dissolved in toluene and filtered through alumina to remove the catalyst. Evaporation of the solvent afforded the dimerisation product.

Data for 6: Colourless oil, yield: 73 mg (98%); ¹H NMR (200.1 MHz, CDCl₃, 25°C): δ = 2.40 (t, ³*J*_{HH} = 7.2 Hz, 4H; C≡CCH₂), 3.48 (t, ³*J*_{HH} = 6.8 Hz, 4H; OCH₂), 4.46 (s, 4H; OCH₂), 7.18–7.29 ppm (m, 10H; ArH); ¹³C NMR (50.3 MHz, CDCl₃, 25°C): δ = 20.2 (s, CH₂), 68.7 (s, OCH₂), 72.9 (s, OCH₂), 77.9 (s, C≡C), 127.5 (s, Ar-C), 127.6 (s, Ar-C), 128.3 (s, Ar-C), 138.2 ppm (s, *i*-C); elemental analysis calcd (%) for C₂₀H₂₂O₂: C 81.60, H 7.53; found: C 81.10, H 7.55.

Data for 8a: White crystalline solid, yield: 78 mg (97%); ¹H NMR (200.1 MHz, CDCl₃, 25°C): δ = 2.57 (t, ³*J*_{HH} = 7.0 Hz, 4H; C≡CCH₂), 4.31 (t, ³*J*_{HH} = 6.8 Hz, 4H; OCH₂), 7.29–7.52 (m, 8H; ArH), 7.97–8.06 ppm (m, 2H; ArH); ¹³C NMR (50.3 MHz, CDCl₃, 25°C): δ = 19.4 (s, CH₂), 63.0 (s, OCH₂), 77.5 (s, C≡C), 128.3 (s, Ar-C), 129.6 (s, Ar-C), 130.1 (s, *i*-C), 133.0 (s, Ar-C), 166.3 ppm (s, C=O); elemental analysis calcd (%) for C₂₀H₂₂O₂: C 74.52, H 5.63; found: C 74.42, H 5.66.

Data for 8b: White crystalline solid, yield: 97 mg (98%); ¹H NMR (200.1 MHz, CDCl₃, 25°C): δ = 2.56 (t, ³*J*_{HH} = 7.0 Hz, 4H; C≡CCH₂), 4.30 (t, ³*J*_{HH} = 6.8 Hz, 4H; OCH₂), 7.27–7.36 (m, 4H; ArH), 7.85–7.93 ppm

(m, 4H; ArH); ¹³C NMR (50.3 MHz, CDCl₃, 25°C): δ = 19.3 (s, CH₂), 63.2 (s, OCH₂), 77.5 (s, C≡C), 128.4 (s, *i*-C), 128.7 (s, Ar-C), 131.0 (s, Ar-C), 133.0 (s, Ar-C), 139.5 (C-Cl), 165.4 ppm (s, C=O); elemental analysis calcd (%) for C₂₀H₂₂O₂: C 61.40, H 4.12; found: C 61.18, H 4.21.

Data for 8c: White crystalline solid, yield: 94 mg (98%); ¹H NMR (200.1 MHz, CDCl₃, 25°C): δ = 2.54 (t, ³*J*_{HH} = 6.9 Hz, 4H; C≡CCH₂), 3.75 (s, 6H; OCH₃), 4.27 (t, ³*J*_{HH} = 6.6 Hz, 4H; OCH₂), 6.77–6.85 (m, 4H; ArH), 7.87–7.94 ppm (m, 4H; ArH); ¹³C NMR (50.3 MHz, CDCl₃, 25°C): δ = 18.7 (s, CH₂), 54.7 (s, OCH₃), 62.1 (s, OCH₂), 76.9 (s, C≡C), 112.9 (s, *i*-C), 121.8 (s, Ar-C), 130.9 (s, Ar-C), 162.7 (s, Ar-C), 165.4 ppm (s, C=O); elemental analysis calcd (%) for C₂₀H₂₂O₂: C 69.1, H 5.8; found: C 69.12, H 5.93.

Data for 8d: White solid, yield: 97 mg (94%); ¹H NMR (200.1 MHz, CDCl₃, 25°C): δ = 2.43 (s, 6H; SCH₃), 2.55 (t, ³*J*_{HH} = 6.9 Hz, 4H; C≡CCH₂), 4.29 (t, ³*J*_{HH} = 6.6 Hz, 4H; OCH₂), 7.11–7.19 (m, 4H; ArH), 7.81–7.91 ppm (m, 4H; ArH); ¹³C NMR (50.3 MHz, CDCl₃, 25°C): δ = 14.1 (s, CH₃), 18.7 (s, CH₂), 62.3 (s, OCH₂), 76.9 (s, C≡C), 124.2 (s, *i*-C), 125.5 (s, Ar-C), 129.2 (s, Ar-C), 144.9 (s, Ar-C), 165.4 ppm (s, C=O); elemental analysis calcd (%) for C₂₀H₂₂O₄S₂: C 63.74, H 5.35, S 15.47; found: C 63.82, H 5.48, S 14.90.

Data for 8e: White solid, yield: 17% based on GC analysis, as no full conversion was achieved; ¹H NMR (200.1 MHz, CDCl₃, 25°C): δ = 2.57 (t, ³*J*_{HH} = 7.1 Hz, 4H; C≡CCH₂), 4.35 (t, ³*J*_{HH} = 6.8 Hz, 4H; OCH₂), 8.09–8.24 ppm (m, 8H; ArH); ¹³C NMR (50.3 MHz, CDCl₃, 25°C): δ = 18.6 (s, CH₂), 63.4 (s, OCH₂), 76.8 (s, C≡C), 122.8 (s, *i*-C), 130.0 (s, Ar-C), 134.6 (s, Ar-C), 149.9 (s, Ar-C), 163.7 ppm (s, C=O); ESI: *m/z* calcd for C₂₀H₁₆N₂O₈+Na: 435.08044; found: 435.07988.

General procedure for ring-closing alkyne metathesis: In a glove box, a 250 mL Schlenk tube was charged with a solution of the substrate (0.55 mmol) and the catalyst **3a** (11 μmol, 2 mol%) in toluene (120 mL). The Schlenk tube was taken out of the glove box and connected to a Schlenk line. Reduced pressure (300 mbar) was applied to remove 2-butyne continuously. Under these conditions, the volume of the toluene solution remained almost constant. After 2 h the solution was filtered through alumina in order to remove the catalyst, and elution with Et₂O afforded the cyclisation product as colourless crystals after evaporation of the solvent.

Data for 10: Yield: 102 mg (86%); ¹H NMR (200.1 MHz, CDCl₃, 25°C): δ = 2.45 (t, ³*J*_{HH} = 5.2 Hz, 4H; C≡CCH₂), 3.65 (t, ³*J*_{HH} = 4.8 Hz, 4H; OCH₂), 4.65 (s, 4H; OCH₂), 7.03 (m, 2H; ArH), 7.27 (m, 1H; ArH), 8.30 ppm (m, 1H; ArH); ¹³C NMR (50.3 MHz, CDCl₃, 25°C): δ = 20.9 (s, CH₂), 68.9 (s, OCH₂), 71.1 (s, OCH₂), 79.5 (s, C≡C), 124.5 (s, Ar-C), 125.0 (s, Ar-C), 127.6 (s, Ar-C), 139.7 ppm (s, *i*-C); elemental analysis calcd (%) for C₁₄H₁₆O₂: C 77.75, H 7.46; found: C 77.66, H 7.70.

Data for 12: Yield: 134 mg (98%); ¹H NMR (200.1 MHz, CDCl₃, 25°C): δ = 2.60 (t, *J* = 5.6 Hz, 4H; C≡CCH₂), 4.51 (t, ³*J*_{HH} = 5.4 Hz, 4H; OCH₂), 7.55–7.64 (m, 2H; ArH), 7.71–7.80 ppm (2H; m, ArH); ¹³C NMR (50.3 MHz, CDCl₃, 25°C): δ = 19.8 (s, CH₂), 62.7 (s, OCH₂), 78.9 (s, C≡C), 128.4 (s, Ar-C), 130.9 (s, Ar-C), 133.2 (s, *i*-C), 167.8 ppm (s, C=O); elemental analysis calcd (%) for C₁₄H₁₂O₄: C 68.85, H 4.95; found: C 68.47, H 4.94.

Single-crystal X-ray structure determination: Data were recorded on an Oxford Diffraction Xcalibur diffractometer at low temperature by using monochromated MoK_α radiation (λ = 0.71073 Å). Absorption corrections (except for **12**) were performed on the basis of multi-scans. Structures were refined anisotropically using the program SHELXL-97. Hydrogen atoms were included using rigid methyl groups or a riding model.

Special features: The Flack parameters for the noncentrosymmetric structures of **3a** and **3b** were refined to -0.015(2) and -0.009(11), respectively. These isotopic compounds crystallised by chance with opposite polarity. In compound **4**, one of the hexafluoro-*tert*-butoxide groups is disordered over two positions; the atoms of the minor component were refined isotropically. For compound **12**, the anomalous dispersion is negligible; Friedel opposite reflections were therefore merged and the Flack parameter is meaningless. Crystallographic data are given in Table 2 for structures **2a**, **2b**, **3a**, **3b**, **4**, and **12**.

Table 2. Crystallographic data.

	2a	2b	3a	3b	4	12
formula	C ₂₂ H ₂₄ F ₁₈ O ₅ W	C ₂₃ H ₂₄ F ₁₈ O ₅ Mo	C ₂₆ H ₃₁ F ₁₂ N ₃ O ₂ W	C ₂₆ H ₃₁ F ₁₂ N ₃ O ₂ Mo	C ₂₂ H ₃₁ F ₁₂ N ₃ O ₂ Mo	C ₁₁ H ₁₂ O ₄
<i>M_r</i>	906.27	818.36	829.39	741.48	693.44	244.24
<i>T</i> [K]	100(2)	100(2)	100(2)	100(2)	100(2)	100(2)
crystal system	triclinic	triclinic	orthorhombic	orthorhombic	orthorhombic	monoclinic
space group	<i>P</i> $\bar{1}$	<i>P</i> $\bar{1}$	<i>P</i> ₂ ₁ ₂ ₁	<i>P</i> ₂ ₁ ₂ ₁	<i>Pbca</i>	<i>P</i> ₂ ₁
<i>a</i> [Å]	10.5640(4)	10.5062(4)	11.285	11.1850(6)	21.7351(3)	8.4753(4)
<i>b</i> [Å]	11.0411(6)	11.0573(6)	20.8290(2)	20.9088(8)	11.9124(2)	7.6964(4)
<i>c</i> [Å]	12.4480(6)	12.4533(6)	39.0341(4)	39.0969(8)	22.0931(3)	9.6504(4)
α [°]	86.572(4)	86.616(4)	90	90	90	90
β [°]	84.574(4)	84.441(4)	90	90	90	109.167(4)
γ [°]	84.859(4)	84.975(4)	90	90	90	90
<i>V</i> [Å ³]	1437.66(12)	1432.50(12)	9175.58(13)	9143.4(6)	5720.28(15)	594.59(5)
<i>Z</i>	2	2	12	8	8	2
crystal size [mm]	0.09 × 0.03 × 0.03	0.21 × 0.14 × 0.13	0.15 × 0.13 × 0.12	0.39 × 0.13 × 0.08	0.26 × 0.06 × 0.04	0.28 × 0.28 × 0.17
2 θ range [°]	2.41–27.10	3.20–28.28	4.34–28.28	2.10–26.37	2.07–26.37	2.23–27.10
reflections collected	39663	29059	189717	174309	121294	13317
independent reflections	6321	7064	22595	18652	5846	1413
goodness of fit on <i>F</i> ²	0.974	1.038	0.958	0.971	0.893	1.109
<i>R</i> (000)	876	812	4872	4488	2800	256
ρ_{calcd} [g cm ⁻³]	2.094	1.897	1.801	1.616	1.610	1.364
μ [mm ⁻¹]	4.169	0.610	3.879	0.533	0.561	0.100
<i>R</i> (<i>F_o</i>), [<i>I</i> > 2 σ (<i>I</i>)]	0.0233	0.0236	0.0182	0.0243	0.0403	0.0239
<i>R_w</i> (<i>F_o</i> ²)	0.0410	0.0650	0.0334	0.0478	0.0943	0.0614
$\Delta\rho$ [e Å ⁻³]	1.174/–0.630	0.758/–0.408	0.958/–0.789	0.454/–0.809	0.967/–0.740	0.170/–0.174

CCDC-768402 (**2a**), 768403 (**2b**), 768404 (**3a**), 768405 (**3b**), 768406 (**4**), and 768407 (**12**) contain the supplementary crystallographic data for this paper. These data can be obtained free of charge from The Cambridge Crystallographic Data Centre via www.ccdc.cam.ac.uk/data_request/cif.

Electronic structure calculations: The B3LYP hybrid functional^[24,25] as implemented in the Gaussian 03^[26] set of programs was employed for all calculations. All atoms except molybdenum and tungsten were described by a standard triple zeta all-electron basis set augmented with one set of polarisation functions (6-311G(d,p)). For molybdenum and tungsten, respectively, a double-zeta basis set optimised for use with effective core potentials (ECP) in combination with the corresponding Stuttgart ECP was employed,^[27] and an additional polarisation function was added ($\xi(f)=1.043$ for molybdenum and $\xi(f)=0.823$ for tungsten).^[28] All geometry optimisations were performed without any imposed symmetry constraints. After the relevant stationary points were localised on the energy surface, they were further characterised as minima or transition states by normal mode analysis based on the analytical energy second derivatives. The self-consistent field iteration was terminated after reaching the convergence criterion of 1×10^{-7} hartree. The root mean square of the internal forces is always below 0.0003 hartreebohr⁻¹. Enthalpic and entropic contributions were calculated by statistical thermodynamics as implemented in the Gaussian 03 set of programs.^[26] Cartesian coordinates of all calculated structures can be found in the Supporting Information.

Acknowledgements

This work was supported by the Deutsche Forschungsgemeinschaft (DFG) through grant Ta 189/6-2.

- [1] For reviews on alkyne metathesis, see: a) W. Zhang, J. S. Moore, *Adv. Synth. Catal.* **2007**, *349*, 93–120; b) R. R. Schrock, C. Czekelius, *Adv. Synth. Catal.* **2007**, *349*, 55–77; c) P. Van de Weghe, P. Bissert, N. Blanchard, J. Eustache, *J. Organomet. Chem.* **2006**, *691*, 5078–5108; d) A. Mortreux, O. Coutelier, *J. Mol. Catal. A* **2006**, *254*, 96–104; e) R. R. Schrock, *Chem. Commun.* **2005**, 2773–2777; f) U. H. F. Bunz, *Science* **2005**, *308*, 216–217; g) R. R. Schrock, *Chem. Rev.* **2002**, *102*, 145–179; h) A. Fürstner, P. Davis, *Chem. Commun.* **2005**,

2307–2320; i) R. R. Schrock, A. H. Hoveyda, *Angew. Chem.* **2003**, *115*, 4740–4782; *Angew. Chem. Int. Ed.* **2003**, *42*, 4592–4633; j) A. Fürstner in *Handbook of Metathesis*, Vol. 2 (Eds.: R. H. Grubbs), Wiley-VCH, Weinheim, **2003**, p. 432.

- [2] a) A. Mortreux, M. Blanchard, *J. Chem. Soc. Chem. Commun.* **1974**, 786–787; b) A. Mortreux, N. Dy, M. Blanchard, *J. Mol. Catal.* **1975**, *1*, 101–109; c) A. Mortreux, F. Petit, M. Blanchard, *Tetrahedron Lett.* **1978**, *19*, 4967–4968; d) A. Bencheick, M. Petit, A. Mortreux, F. Petit, *J. Mol. Catal.* **1982**, *15*, 93–101; e) A. Mortreux, J. C. Delgrange, M. Blanchard, B. Lubochinsky, *J. Mol. Catal.* **1977**, *2*, 73–82; f) A. Mortreux, F. Petit, M. Blanchard, *J. Mol. Catal.* **1980**, *8*, 97–106; g) N. Kaneta, K. Hikichi, M. Mori, *Chem. Lett.* **1995**, 1055–1066; h) W. Zhang, J. S. Moore, *Angew. Chem.* **2006**, *118*, 4524–4548; *Angew. Chem. Int. Ed.* **2006**, *45*, 4416–4439; i) D. Zhao, J. S. Moore, *Chem. Commun.* **2003**, 807–818; j) G. Brizius, N. G. Pschirer, W. Steffen, K. Stitzer, H.-C. zur Loye, U. H. F. Bunz, *J. Am. Chem. Soc.* **2000**, *122*, 12435–12440; k) P.-H. Ge, W. Fu, W. A. Herrmann, E. Herdtweck, C. Campana, R. D. Adams, U. H. F. Bunz, *Angew. Chem.* **2000**, *112*, 3753–3756; *Angew. Chem. Int. Ed.* **2000**, *39*, 3607–3610; l) S. Höger, *Angew. Chem.* **2005**, *117*, 3872–3875; *Angew. Chem. Int. Ed.* **2005**, *44*, 3806–3808; m) O. S. Miljanic, K. P. C. Vollhardt, G. D. Whitener, *Synlett* **2003**, 29; n) C. A. Johnson II, Y. Lu, M. M. Haley, *Org. Lett.* **2007**, *9*, 3725–3728; o) A. Fürstner, O. Guth, A. Rumbo, G. Seidel, *J. Am. Chem. Soc.* **1999**, *121*, 11108–11113.
- [3] a) J. Sancho, R. R. Schrock, *J. Mol. Catal.* **1982**, *15*, 75–79; b) R. R. Schrock, D. N. Clark, J. Sancho, J. H. Wengrovius, S. M. Rocklage, S. F. Pederson, *Organometallics* **1982**, *1*, 1645–1651; c) J. H. Wengrovius, J. Sancho, R. R. Schrock, *J. Am. Chem. Soc.* **1981**, *103*, 3932–3934; d) A. Fürstner, G. Seidel, *Angew. Chem.* **1998**, *110*, 1758–1760; *Angew. Chem. Int. Ed.* **1998**, *37*, 1734–1736; e) K. Grela, J. Ignatowska, *Org. Lett.* **2002**, *4*, 3747–3749; f) D. Song, G. Blond, A. Fürstner, *Tetrahedron* **2003**, *59*, 6899–6904; g) A. Fürstner, G. Müller, *J. Organomet. Chem.* **2000**, *606*, 75–78.
- [4] a) C. E. Laplaza, A. L. Odom, W. M. Davis, C. C. Cummins, J. D. Protasiewicz, *J. Am. Chem. Soc.* **1995**, *117*, 4999–5000; b) C. E. Laplaza, C. C. Cummins, *Science* **1995**, *268*, 861–863; c) C. E. Laplaza, A. R. Johnson, C. C. Cummins, *J. Am. Chem. Soc.* **1996**, *118*, 709–710; d) A. Fürstner, C. Mathes, C. W. Lehmann, *J. Am. Chem. Soc.* **1999**, *121*, 9453–9454; e) A. Fürstner, C. Mathes, C. W. Lehmann,

- Chem. Eur. J.* **2001**, *7*, 5299–5317; f) Y.-C. Tsai, P. L. Diaconescu, C. C. Cummins, *Organometallics* **2000**, *19*, 5260–5262; g) J. M. Blackwell, J. S. Figueroa, F. H. Stephens, C. C. Cummins, *Organometallics* **2003**, *22*, 3351–3353; h) W. Zhang, S. Kraft, J. S. Moore, *Chem. Commun.* **2003**, 832–833; i) W. Zhang, S. Kraft, J. S. Moore, *J. Am. Chem. Soc.* **2004**, *126*, 329–335; j) W. Zhang, J. S. Moore, *J. Am. Chem. Soc.* **2005**, *127*, 11863–11870; k) W. Zhang, J. S. Moore, *J. Am. Chem. Soc.* **2004**, *126*, 12796; l) W. Zhang, M. Brombosz, J. L. Mendoza, J. S. Moore, *J. Org. Chem.* **2005**, *70*, 10198–10201; m) H. M. Cho, H. Weissmann, J. S. Moore, *J. Org. Chem.* **2008**, *73*, 4256–4258; n) H. Weissman, K. N. Plunkett, J. S. Moore, *Angew. Chem.* **2006**, *118*, 599–602; *Angew. Chem. Int. Ed.* **2006**, *45*, 585–588.
- [5] a) M. Bindl, R. Stade, E. K. Heilmann, A. Picot, R. Goddard, A. Fürstner, *J. Am. Chem. Soc.* **2009**, *131*, 9468–9470; b) M. Bindl, L. Jean, J. Herrmann, R. Müller, A. Fürstner, *Chem. Eur. J.* **2009**, *15*, 12310–12319.
- [6] a) S. Beer, C. G. Hrib, P. G. Jones, K. Brandhorst, J. Grunenberg, M. Tamm, *Angew. Chem.* **2007**, *119*, 9047–9051; *Angew. Chem. Int. Ed.* **2007**, *46*, 8890–8894; b) M. Tamm, S. Beer, T. Bannenberg, EP 07112300.4; c) S. Beer, K. Brandhorst, C. G. Hrib, X. Wu, B. Haberlag, J. Grunenberg, P. G. Jones, M. Tamm, *Organometallics* **2009**, *28*, 1534–1545; d) M. Tamm, X. Wu, *Chim. Oggi* **2010**, *28*, 10–13.
- [7] a) S. Beer, K. Brandhorst, J. Grunenberg, C. G. Hrib, P. G. Jones, M. Tamm, *Org. Lett.* **2008**, *10*, 981–984; b) S. Lysenko, B. Haberlag, X. Wu, M. Tamm, *Macromol. Symp.* **2010**, in press.
- [8] a) M. Tamm, D. Petrovic, S. Randoll, S. Beer, T. Bannenberg, P. G. Jones, J. Grunenberg, *Org. Biomol. Chem.* **2007**, *5*, 523–530; b) M. Tamm, S. Randoll, T. Bannenberg, E. Herdtweck, *Chem. Commun.* **2004**, 876–877; c) M. Tamm, S. Beer, E. Herdtweck, *Z. Naturforsch. B* **2004**, *59*, 1497–1504; d) M. Tamm, S. Randoll, E. Herdtweck, N. Kleigewe, G. Kehr, G. Erker, B. Rieger, *Dalton Trans.* **2006**, 459–467; e) T. K. Panda, S. Randoll, C. G. Hrib, P. G. Jones, T. Bannenberg, M. Tamm, *Chem. Commun.* **2007**, 5007–5009; f) S. H. Stelzig, M. Tamm, R. M. Waymouth, *J. Polym. Sci. Polym. Chem. Ed.* **2008**, *46*, 6064–6070.
- [9] a) A. Mayr, G. A. McDermott, *J. Am. Chem. Soc.* **1986**, *108*, 548–549; b) G. A. McDermott, A. M. Dorries, A. M. Mayr, *Organometallics* **1987**, *6*, 925–931; c) A. Mayr, G. A. McDermott, A. M. Dorries, *Organometallics* **1985**, *4*, 608–610; d) M. A. Stevenson, M. D. Hopkins, *Organometallics* **1997**, *16*, 3572–3573.
- [10] E. O. Fischer, A. Maasböl, *Chem. Ber.* **1967**, *100*, 2445–2456.
- [11] a) S. T. Diver, A. J. Giessert, *Chem. Rev.* **2004**, *104*, 1317–1382; b) E. O. Fischer, G. Kreis, *Chem. Ber.* **1976**, *109*, 1673–1683; c) E. O. Fischer, N. Q. Dao, W. R. Wagner, *Angew. Chem.* **1978**, *90*, 51–51; *Angew. Chem. Int. Ed. Engl.* **1978**, *17*, 50–51; d) E. O. Fischer, U. Schubert, *J. Organomet. Chem.* **1975**, *100*, 59–81.
- [12] J. H. Freudenberger, R. R. Schrock, M. R. Churchill, A. L. Rheingold, J. W. Ziller, *Organometallics* **1984**, *3*, 1563–1573.
- [13] a) T. M. Trnka, R. H. Grubbs, *Acc. Chem. Res.* **2001**, *34*, 18–29; b) A. Deiters, S. F. Martin, *Chem. Rev.* **2004**, *104*, 2199–2238; c) S. J. Connon, S. Blechert, *Angew. Chem.* **2003**, *115*, 1944–1968; *Angew. Chem. Int. Ed.* **2003**, *42*, 1900–1923; d) A. Fürstner, *Angew. Chem.* **2000**, *112*, 3140–3172; *Angew. Chem. Int. Ed.* **2000**, *39*, 3012–3043; e) M. R. Buchmeiser, *Chem. Rev.* **2000**, *100*, 1565–1604; f) M. R. Buchmeiser, *Adv. Polym. Sci.* **2005**, *176*, 89–119; k) M. R. Buchmeiser, *Monatsh. Chem.* **2003**, *134*, 327–342; g) *Handbook of Metathesis, Vol. 1–3* (Eds.: R. H. Grubbs), Wiley-VCH, Weinheim, **2003**; h) A. Fürstner, *Alkene Metathesis in Organic Synthesis*, Springer, Berlin, **1998**; i) S. Monsaert, A. Lozano Vila, R. Drozdak, P. Van Der Voort, F. Verpoort, *Chem. Soc. Rev.* **2009**, *38*, 3360–3372; j) C. Samojłowicz, M. Bieniek, K. Grela, *Chem. Rev.* **2009**, *109*, 3708–3742.
- [14] a) D. N. Clark, R. R. Schrock, *J. Am. Chem. Soc.* **1978**, *100*, 6774–6776; b) L. G. McCullough, R. R. Schrock, J. C. Dewan, J. C. Murdzek, *J. Am. Chem. Soc.* **1985**, *107*, 5987–5998; c) L. G. McCullough, R. R. Schrock, *J. Am. Chem. Soc.* **1984**, *106*, 4067–4068.
- [15] It should be noted, however, that Cummins has provided an improved protocol for the preparation of non-fluorinated trialkoxymolybdenum(VI) alkylidyne complexes, see ref. [4f]; furthermore Johnson has published the synthesis of fluorinated trialkoxymolybdenum(VI) alkylidyne complexes from nitrides by metathesis with alkynes, see: R. L. Gdula, M. J. A. Johnson, *J. Am. Chem. Soc.* **2006**, *128*, 9614–9615.
- [16] R. D. Shannon, *Acta Crystallogr. Sect. A* **1976**, *32*, 751–767.
- [17] a) R. R. Schrock, J. Y. Jamieson, J. P. Araujo, P. J. Bonitatebus, A. Sinha, L. P. H. Lopez, *J. Organomet. Chem.* **2003**, *684*, 56–67; b) R. R. Schrock, *Polyhedron* **1995**, *14*, 3177–3195.
- [18] Using 2 mol % of **3a**, 33 % of **8e** can be obtained.
- [19] K. Brandhorst, J. Grunenberg, M. Tamm, unpublished results; see ref. [7a] for representative calculations.
- [20] a) G. Bocelli, M. F. Grenier-Loustalot, *J. Crystallogr. Spectrosc. Res.* **1983**, *13*, 19–29; b) V. Königstein, W. Tochtermann, E.-M. Peters, K. Peters, H. G. von Schnering, *Tetrahedron Lett.* **1987**, *28*, 3483–3486; c) M. Balog, I. Grosu, G. Plé, Y. Ramondenc, E. Condamine, R. A. Varga, *J. Org. Chem.* **2004**, *69*, 1337–1345.
- [21] T. J. Katz, J. McGinnis, *J. Am. Chem. Soc.* **1975**, *97*, 1592–1594.
- [22] J. Zhu, G. Jia, Z. Lin, *Organometallics* **2006**, *25*, 1812–1819.
- [23] A. Poater, X. Solans-Monfort, E. Clot, C. Copèret, O. Eisenstein, *J. Am. Chem. Soc.* **2007**, *129*, 8207–8216.
- [24] A. D. Becke, *Phys. Rev. B* **1988**, *38*, 3098–3100.
- [25] C. Lee, W. Yang, R. G. Parr, *Phys. Rev. B* **1988**, *37*, 785–789.
- [26] Gaussian 03, Revision E.01, M. J. Frisch, G. W. Trucks, H. B. Schlegel, G. E. Scuseria, M. A. Robb, J. R. Cheeseman, J. A. Montgomery, Jr., T. Vreven, K. N. Kudin, J. C. Burant, J. M. Millam, S. S. Iyengar, J. Tomasi, V. Barone, B. Mennucci, M. Cossi, G. Scalmani, N. Rega, G. A. Petersson, H. Nakatsuji, M. Hada, M. Ehara, K. Toyota, R. Fukuda, J. Hasegawa, M. Ishida, T. Nakajima, Y. Honda, O. Kitao, H. Nakai, M. Klene, X. Li, J. E. Knox, H. P. Hratchian, J. B. Cross, V. Bakken, C. Adamo, J. Jaramillo, R. Gomperts, R. E. Stratmann, O. Yazyev, A. J. Austin, R. Cammi, C. Pomelli, J. W. Ochterski, P. Y. Ayala, K. Morokuma, G. A. Voth, P. Salvador, J. J. Dannenberg, V. G. Zakrzewski, S. Dapprich, A. D. Daniels, M. C. Strain, O. Farkas, D. K. Malick, A. D. Rabuck, K. Raghavachari, J. B. Foresman, J. V. Ortiz, Q. Cui, A. G. Baboul, S. Clifford, J. Cioslowski, B. B. Stefanov, G. Liu, A. Liashenko, P. Piskorz, I. Komaromi, R. L. Martin, D. J. Fox, T. Keith, M. A. Al-Laham, C. Y. Peng, A. Nanayakkara, M. Challacombe, P. M. W. Gill, B. Johnson, W. Chen, M. W. Wong, C. Gonzalez, J. A. Pople, Gaussian Inc., Wallingford CT, **2004**.
- [27] D. Andrae, U. Häußermann, M. Dolg, H. Stoll, H. Preuß, *Theor. Chim. Acta* **1990**, *77*, 123–141.
- [28] A. W. Ehlers, M. Bohme, S. Dapprich, A. Gobbi, A. Hollwarth, V. Jonas, K. F. Kohler, R. Stegmann, A. Veldkamp, G. Frenking, *Chem. Phys. Lett.* **1993**, *208*, 111–114.

Received: March 7, 2010
Published online: June 22, 2010